

# PROCEEDINGS OF SPIE

[SPIDigitalLibrary.org/conference-proceedings-of-spie](https://SPIDigitalLibrary.org/conference-proceedings-of-spie)

## Device for measuring stress stability in reflective coatings for thin x-ray mirrors

Mallory Whalen, Ralf Heilmann, Mark Schattenburg

Mallory M. Whalen, Ralf K. Heilmann, Mark L. Schattenburg, "Device for measuring stress stability in reflective coatings for thin x-ray mirrors," Proc. SPIE 12679, Optics for EUV, X-Ray, and Gamma-Ray Astronomy XI, 126790P (5 October 2023); doi: 10.1117/12.2677492

**SPIE.**

Event: SPIE Optical Engineering + Applications, 2023, San Diego, California, United States

# Device for Measuring Stress Stability in Reflective Coatings for Thin X-Ray Mirrors

Mallory M. Whalen<sup>a,b</sup>, Ralf K. Heilmann<sup>a</sup>, and Mark L. Schattenburg<sup>a</sup>

<sup>a</sup>Space Nanotechnology Laboratory, Kavli Institute for Astrophysics and Space Research,  
Massachusetts Institute of Technology, Cambridge, MA, USA

<sup>b</sup>Department of Mechanical Engineering, Massachusetts Institute of Technology, Cambridge,  
MA, USA

## ABSTRACT

A novel device that uses the membrane resonance method of measuring stress in thin films to track the stress stability of candidate X-ray reflective coatings is presented. The device is capable of tracking stress changes below 0.1 N/m, which is the threshold where stress-based mirror deformations and resulting degradation of angular resolution can become problematic for next-generation X-ray observatories. The device can be used to determine optimal coatings by evaluating the stress stability of different metals and heat treatments.

**Keywords:** Coatings, stress, stability, segmented optics

## 1. INTRODUCTION

Next-generation X-ray observatories aim to achieve high angular resolution of at least 0.5 arc-seconds half-power diameter (HPD) while increasing effective collecting area. The segmented mirror approach uses thousands of thin silicon mirrors with X-ray reflective metallic coatings to reach these goals while keeping mass low. The lightweight optics are highly sensitive to figure deformation from the stress in their X-ray reflective coatings [1]. The prevention and correction of mirror figure error after coating with x-ray reflective coatings has been well studied for segmented optics. However, the stability of the stress in the coating receives little attention. We present a novel use of the membrane resonance method of measuring thin film stress and describe a device that uses the method to repeatably measure thin film stress over long time periods.

The typical X-ray reflective coatings, such as gold, platinum, or iridium, used on X-ray optics at a thickness of 15 nm typically exhibit a high compressive stress of more than 1 GPa. It is known that these coatings are capable of deforming lightweight X-ray mirrors, thus degrading the resolution of the telescope [2–4].

Finite element analysis done by Chalifoux has shown that a 0.1 N/m compressive integrated stress (approximately 7 MPa  $\times$  15 nm) change in an iridium coating on all mirrors (100 mm length,  $\sim$ 100 mm width, and 0.5 mm thickness) in a meta shell telescope can degrade the total resolution by 0.115 arc sec HPD [5]. The outermost mirrors of the largest radius are most affected by this stress change. A top-level angular resolution error budget given by Zhang in 2019 states that the coating must not degrade the point spread function of the mirror pair by more than 0.1 arc sec [1].

## 2. BACKGROUND

### 2.1 Thin Film Stress

Thin film stress,  $\sigma_f$  (N/m<sup>2</sup>), typically has two characteristics. The first is that the film thickness,  $h_f$  (m), is much thinner than the substrate thickness,  $h_s$  (m). The second is that the stress state in the film is equibiaxial, meaning that the in-plane principal stresses are equal and that there are no shear stresses. X-ray mirror coatings are around 15 – 30 nm thick, while the silicon mirrors are about 0.5 mm thick. Intrinsic film stress from amorphous or polycrystalline films is usually equibiaxial. To avoid ambiguity in cases where the film thickness

---

Further author information: (Send correspondence to M.M.W.)  
E-mail: malw at mit.edu

is nonuniform or the film stress varies as an unknown function of height,  $z$  (m), integrated stress,  $N_f$  (N/m), is used to describe the stress in the film. Integrated stress is calculated as:

$$N_f = \int_z \sigma_f dz \approx \sigma_f h_f \quad (1)$$

## 2.2 Thin Film Growth

Thin film stress arises during deposition. Magnetron sputtering is the most common deposition method for X-ray reflective coatings. Metals deposited on silicon usually form through the Volmer-Webber growth mechanism, discussed and simulated by Seel. Islands of atoms form, grow, and then impinge upon each other, and finally coalesce to form a polycrystalline thin film [6]. There are two growth regimes that occur as the film thickens. Abermann discussed these regimes and showed that thin films exhibit two different types of stress versus thickness curves during deposition and classifies them as type I or type II. Type I materials, materials with low adatom mobility, show a monotonic increase in tensile stress with thickness. They have a columnar grain structure, which results in high surface roughness. Type II materials, materials with high adatom mobility, exhibit a compressive-tensile-compressive stress change as more atoms are deposited during deposition. Type II materials display an equiaxed grain structure which results in lower surface roughness [7,8]. In type II materials, islands of atoms form, and the stress is compressive. Then, tensile stresses arise from the coalescence of islands and increase from the creation and growth of grain boundaries. Finally, the stress becomes compressive again due to the diffusion of adatoms into the grain boundaries [6]. After deposition, tensile stress is generated in the film due to the thermal mismatch between the cooled substrate and film [9]. Deposition parameters, such as plasma gas pressure and substrate temperature, influence the stress profile and magnitude as well as the film density and roughness [10]. Additionally, Thornton identified intermediate grain structures which will not be discussed here [11].

## 2.3 Stress Change in X-Ray Reflective Coatings

Thin films are not in stress equilibrium after deposition. Grain size, defect structure, and crystal structure can all change to reduce energy [9,12]. In coated mirrors, plastic deformation in the thin coatings accounts for all the stress relaxation and, thus, mirror figure change. Stress relaxation and creep in thin films occurs due to a variety of mechanisms, which are summarized by Gall [9]. Additionally, water absorption into the porous films has been shown to cause stress change [10,13].

The X-ray mirror community has used high temperature thermal annealing to “stabilize” thin films [4,14]. Thermal annealing helps create a more stable grain structure through grain growth and crystallization [12]. However, there is no study showing that film relaxation remains under 0.1 N/m after annealing candidate X-ray reflective coatings.

## 2.4 Existing Substrate Curvature Measurement Techniques

The substrate curvature method of measuring integrated stress is the standard measurement technique. Substrate curvature methods use the Stoney equation to relate substrate curvature to thin film stress [15]. The Stoney equation for plates is:

$$\sigma_f h_f = \frac{E h_s^2}{6(1 - \nu_s)} \Delta\kappa \quad (2)$$

$E$  (Pa) is the Young’s Modulus of the substrate,  $\Delta\kappa$  (1/m) is the curvature change of the sample, and Poisson’s ratio of the substrate is  $\nu_s$ . The quantity  $\sigma_f h_f$ , the film stress times the film thickness (integrated stress) in units of N/m, is what is responsible for the substrate curvature. However, the stress measurement repeatability is limited due to unintended deformations caused during substrate mounting and noise from vibration.

Several substrate curvature measurement devices exist. Optical and stylus-based measurements of silicon wafers and thin cantilevers are commonly implemented. Multiple beams, such as those used in the technique called multiple beam optical stress sensor (MOSS), reduce the measurement’s sensitivity to substrate vibration

[16,17]. MOSS is fundamentally limited by pixel accuracy in measuring beam displacements [18]. Additionally, as can be seen from the exponential in the Stoney equation, substrate thickness limits film stress sensitivity. The MOS UltraScan from kSa has a 0.32 N/m repeatability, which they define as the standard deviation of stress across 10 scans. This is the same as the tool's stress resolution, 0.32 N/m [19]. It is unclear if they remount the wafer between scans; this is a factor which can dramatically reduce repeatability due to loading from thermal stress, frictional force, and gravity sag. A low distortion thin optics mount that measures optic curvature with a Shack-Hartmann wavefront sensor was found to have a stress measurement repeatability of  $\pm 1$  N/m when the wafer is remounted after each measurement [20,21]. For the target maximum film stress change of 0.1 N/m to be measured, the repeatability of the measurement system should be about 10% of the target value, i.e. 0.01 N/m repeatability. Existing techniques are not capable of measuring at this repeatability.

### 3. MEMBRANE RESONANCE TECHNIQUE

The resonant frequency of coated membranes can be used to determine thin film stress. The membrane resonance method was explored in the early 1990s when X-ray lithography masks, made of thin silicon membranes, were being developed, and was also used for *in-situ* thin film stress measurements around this time [22–28]. The stress sensitivity of the technique is said to be 0.001 N/m [28].

As in strings, the resonant frequency of membranes depends on the in-plane tension and the density. Lord Rayleigh idealized the membrane as perfectly flexible, infinitely thin, and stretched in all directions by a tension that is negligibly changed during vibration [29]. Adapting Rayleigh's derivation to include a membrane with a thin coating provides the resonant frequency of a coated circular membrane [24,30]:

$$f = \frac{1}{2.61a} \sqrt{\frac{N_m + N_f}{\rho_m h_m + \rho_f h_f}}, \quad (3)$$

where  $f$  (Hz) is the resonant frequency (first mode),  $a$  (m) is the membrane radius,  $N$  (N/m) is the integrated stress,  $\rho$  (kg/m<sup>3</sup>) is the density, and  $h$  (m) is the thickness. The subscripts  $m$  and  $f$  refer to the membrane and the film, respectively. This equation applies to uncoated membranes as well, where the terms with subscript  $f$  drop out. The  $N_m$  term is the residual stress in the membrane. Residual stress is created during membrane fabrication. For example, boron doping in silicon membranes shrinks the lattice and causes a residual tensile stress in the membrane [26].

### 4. DEVICE DESIGN

This study adapts the membrane resonance technique from an *in-situ* measurement to one that can be used to track the stability of coatings over long time periods. The modeling and design of the device is described in detail by Whalen [31].

The device electrostatically actuates a membrane and measures its vibrational amplitude with a laser Doppler vibrometer (LDV). The Polytec VibroGo was used in this study. The doped membrane acts as the flexible electrode in a variable gap capacitor. The resonant frequency can be found by plotting vibrational amplitude versus actuation frequency. Air can greatly damp the resonant amplitude of a membrane and reduce the sensitivity of the stress measurement. The experimental setup is in a vacuum chamber that pumps down to  $10^{-5}$  to  $10^{-6}$  torr to minimize the effects of air.

The membranes used are 2  $\mu\text{m}$  thick, 6 mm diameter, highly boron-doped silicon membranes etched into 300  $\mu\text{m}$ -thick frames. The boron doping has a 0.01  $\Omega\text{cm}$  to 0.02  $\Omega\text{cm}$  resistivity. Devices were fabricated by Norcada.

The silicon frame is fixtured on a special borosilicate glass holder which is then fixtured inside a vacuum flange on a linear slide. The borosilicate glass holder allows electrical connection to the membrane and electrode. It is a two-part design, comprised of a 500  $\mu\text{m}$  thick borosilicate glass wafer and 5 mm thick borosilicate glass blank. Conductive silver adhesive bonds the two pieces together and creates electrical traces that run off the side of the glass blank. A  $178 \pm 9$   $\mu\text{m}$  thick, 5.9 mm diameter steel circle cut from shim stock acts as the electrode. The silicon frame sits completely on borosilicate glass.

The borosilicate glass holder is held in the vacuum chamber by means of a kinematic holder. It sits on three borosilicate glass balls and is positioned against three ceramic posts. Two of the posts are coated with silver adhesive and form an electrical connection with the traces on the glass holder. A flexure provides preload to keep the glass holder in contact with the posts used for the electrical connection. Figure 1 shows the device. The vacuum chamber is kept in a temperature-controlled environment on a vibration isolation table.

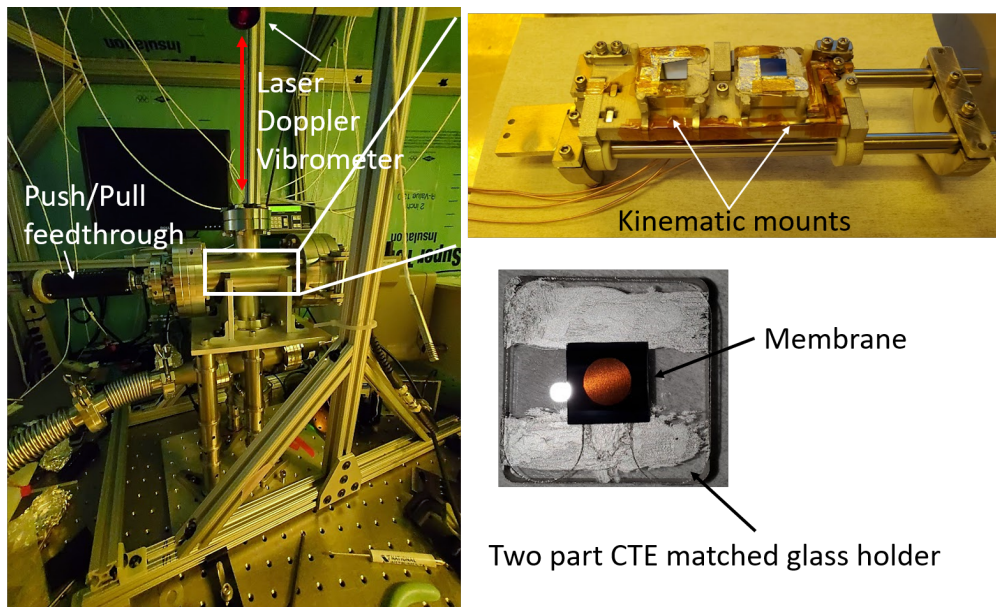


Figure 1. Experimental setup showing the glass holder, kinematic mounting of the glass holders on a linear slide, and the vacuum flange that the linear slide sits in. A push/pull feedthrough actuates the slide to position either membrane for measurement with the laser Doppler vibrometer.

## 5. STABILITY TESTING

### 5.1 Uncoated Membrane

The stability of the uncoated membrane was tested. An uncoated membrane was left in the kinematic holder and its resonant frequency was recorded over the period of a week. The membrane was kept at atmospheric pressure between tests. A 1 O.D. optical filter was placed over the viewport window to reduce heating from the laser. The mean resonant frequency across the tests was  $5363.9 \pm 1.4$  Hz, which corresponds to a mean stress of  $8.220 \pm 0.004$  N/m. Figure 2 shows the frequency sweeps. Temperature fluctuations in the temperature-controlled environment were  $\pm 0.01$  °C.

Preliminary testing for integrated stress repeatability - when the glass holder is taken out of the vacuum chamber and remounted - was performed. Four different trials were done. The membrane was measured on the first trial and then remounted on each subsequent trial. The mean integrated stress was  $8.275 \pm 0.034$  N/m (this test was done with a 3 O.D. filter). The added non-repeatability is believed to be dominated by slight changes in the laser position on the membrane that results in different membrane heating.

### 5.2 Coated Membrane

A 5 nm gold layer was sputter deposited onto a membrane at room temperature. As the coating is so thin, stress relaxation was not expected due to the likely absence of grain boundaries. An uncoated membrane was also tested during this time. Both membranes remained in the chamber at atmospheric pressure between tests. Figure 3 shows the stress measurements taken over this time. The mean stress in the gold coated membrane was  $11.367 \pm 0.008$  N/m, and the mean stress in the uncoated membrane was  $8.227 \pm 0.010$  N/m. Note that the uncoated membrane, measured in April as shown in Figure 2 and measured in August as shown in Figure 3, did not see a stress change of significance during storage.

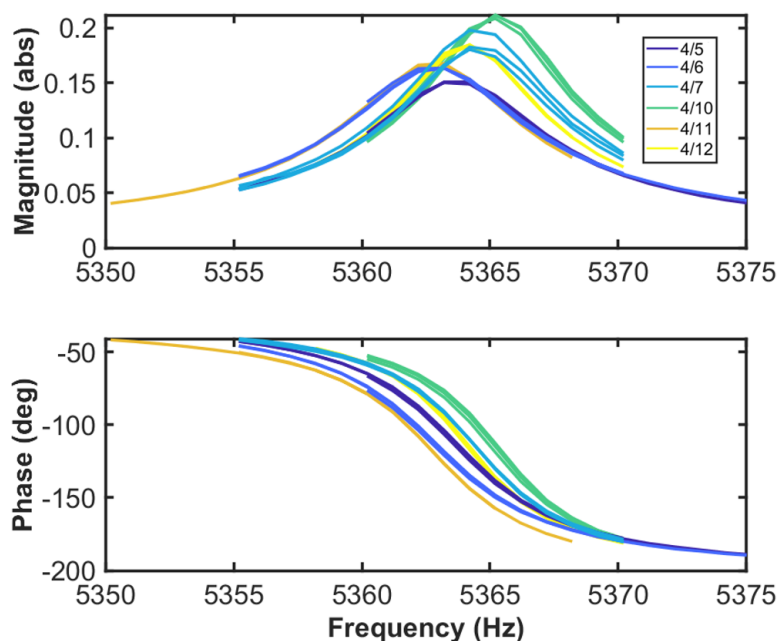


Figure 2. Frequency sweeps of an uncoated membrane performed over a week. Each color represents a different day of testing. The mean resonant frequency across the tests was  $5363.9 \pm 1.4$  Hz, which corresponds to a mean stress of  $8.220 \pm 0.004$  N/m.

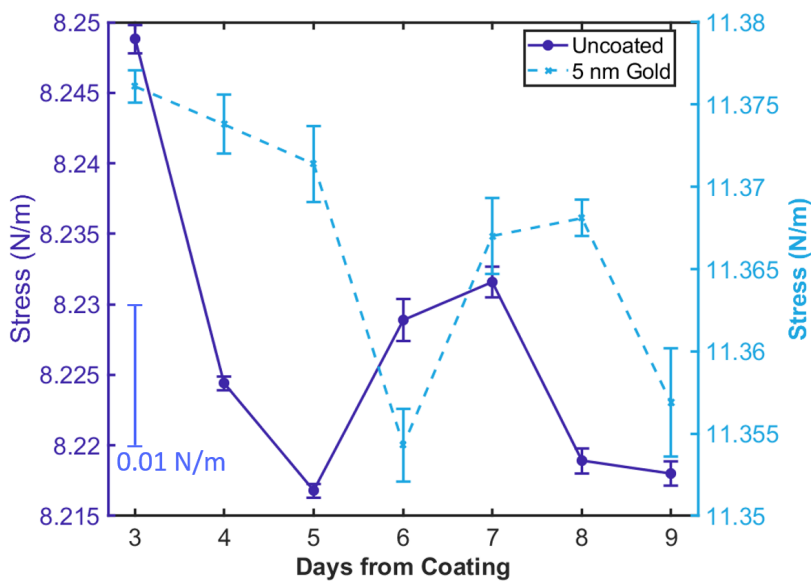


Figure 3. Stress (N/m) of a membrane coated with 5 nm of gold and stress of an uncoated membrane during same week-long period measured in days after coating of the gold membrane. The mean stress in the gold coated membrane was  $11.367 \pm 0.008$  N/m, and the mean stress in the uncoated membrane was  $8.227 \pm 0.010$  N/m. As the gold layer was thin, stress change was not anticipated.

## 6. CONCLUSION

A novel device to measure the stress stability of X-ray reflective coatings to sub 0.1 N/m repeatability has been presented. The repeatability is at least 10 times better than existing measurement techniques. The membrane resonance technique of measuring thin film stress was adapted from its original use as an *in-situ* technique. Thermal fluctuations and laser position change are attributed as the main causes of non-repeatability in the device. In the future, we plan to test this device with thicker coatings and to study the stability of annealed coatings.

## ACKNOWLEDGMENTS

This work was funded by NASA grant 80NSSC20K0907.

## REFERENCES

- [1] Zhang, W. W., 2019, "High-Resolution, Lightweight, and Low-Cost X-Ray Optics for the Lynx Observatory," *JATIS*, **5**(2), p. 021012.
- [2] Serlemitsos, P. J., Ogasaka, Y., Soong, Y., and Chan, K.-W., 1997, "Multilayer Option for Conical Foil X-Ray Mirrors," *Grazing Incidence and Multilayer X-Ray Optical Systems*, SPIE, pp. 244–252.
- [3] Zhang, W. W., Bolognese, J., Byron, G., Chan, K. W., Content, D. A., Hadjimichael, T. J., He, C., Hill, M. D., Hong, M., Lehan, J. P., Lozipone, L., Mazzarella, J. M., McClelland, R., Nguyen, D. T., Olsen, L., Petre, R., Robinson, D., Rohrbach, S. O., Russell, R., Saha, T. T., Sharpe, M., Gubarev, M. V., Jones, W. D., O'Dell, S. L., Davis, W., Caldwell, D. R., Freeman, M., Podgorski, W., and Reid, P. B., 2008, "Constellation-X Mirror Technology Development," *Space Telescopes and Instrumentation 2008: Ultraviolet to Gamma Ray*, SPIE, pp. 43–52.
- [4] Chan, K.-W., Sharpe, M., Zhang, W., Kolos, L., Hong, M., McClelland, R., Hohl, B., Saha, T., and Mazzarella, J., 2013, "Coating Thin Mirror Segments for Lightweight X-Ray Optics," *Optics for EUV, X-Ray, and Gamma-Ray Astronomy VI*, SPIE, pp. 339–350.
- [5] Chalifoux, B. D., Yao, Y., Heilmann, R. K., and Schattenburg, M. L., 2019, "Simulations of Film Stress Effects on Mirror Segments for the Lynx X-Ray Observatory Concept," *JATIS*, **5**(2), p. 021004.
- [6] Seel, S. C., 2002, "Stress and Structure Evolution during Volmer-Weber Growth of Thin Films," Thesis, Massachusetts Institute of Technology.
- [7] Abermann, R., 1990, "Measurements of the Intrinsic Stress in Thin Metal Films," *Vacuum*, **41**(4), pp. 1279–1282.
- [8] Thornton, J. A., and Hoffman, D. W., 1989, "Stress-Related Effects in Thin Films," *Thin Solid Films*, **171**(1), pp. 5–31.
- [9] Gall, K., West, N., Spark, K., Dunn, M. L., and Finch, D. S., 2004, "Creep of Thin Film Au on Bimaterial Au/Si Microcantilevers," *Acta Materialia*, **52**(8), pp. 2133–2146.
- [10] Windischmann, H., 1992, "Intrinsic Stress in Sputter-Deposited Thin Films," *Critical Reviews in Solid State and Materials Sciences*, **17**(6), pp. 547–596.
- [11] Thornton, J. A., 1974, "Influence of Apparatus Geometry and Deposition Conditions on the Structure and Topography of Thick Sputtered Coatings," *Journal of Vacuum Science and Technology*, **11**(4), pp. 666–670.
- [12] Nix, W. D., 1989, "Mechanical Properties of Thin Films," *Metall Mater Trans A*, **20**(11), pp. 2217–2245.
- [13] Guan, D., Bruccoleri, A. R., Heilmann, R. K., and Schattenburg, M. L., 2013, "Stress Control of Plasma Enhanced Chemical Vapor Deposited Silicon Oxide Film from Tetraethoxysilane," *J. Micromech. Microeng.*, **24**(2), p. 027001.
- [14] Yao, Y., Chalifoux, B. D., Heilmann, R. K., and Schattenburg, M. L., 2019, "Thermal Oxide Patterning Method for Compensating Coating Stress in Silicon Substrates," *Opt. Express*, OE, **27**(2), pp. 1010–1024.
- [15] Janssen, G. C. A. M., Abdalla, M. M., van Keulen, F., Pujada, B. R., and van Venrooy, B., 2009, "Celebrating the 100th Anniversary of the Stoney Equation for Film Stress: Developments from Polycrystalline Steel Strips to Single Crystal Silicon Wafers," *Thin Solid Films*, **517**(6), pp. 1858–1867.
- [16] Schell-Sorokin, A. J., and Tromp, R. M., 1990, "Mechanical Stresses in (Sub)Monolayer Epitaxial Films," *Phys. Rev. Lett.*, **64**(9), pp. 1039–1042.

- [17] Chason, E., and Floro, J. A., 1996, “Measurements Of Stress Evolution During Thin Film Deposition,” *MRS Online Proceedings Library (OPL)*, **428**, p. 499.
- [18] Grachev, S., Hérault, Q., Wang, J., Balestrieri, M., Montigaud, H., Lazzari, R., and Gozhyk, I., 2022, “A New Method for High Resolution Curvature Measurement Applied to Stress Monitoring in Thin Films,” *Nanotechnology*, **33**(18), p. 185701.
- [19] “Product Specifications: KSA MOS UltraScan,” k-Space Associates, Inc. [Online]. Available: <https://k-space.com/document/product-specifications-ksa-mos-ultrascan/>. [Accessed: 26-Apr-2023].
- [20] Akilian, M., 2004, “Thin Optic Surface Analysis for High Resolution X-Ray Telescopes,” Thesis, Massachusetts Institute of Technology.
- [21] Chalifoux, B., Sung, E., Heilmann, R. K., and Schattenburg, M. L., 2013, “High-Precision Figure Correction of X-Ray Telescope Optics Using Ion Implantation,” *Optics for EUV, X-Ray, and Gamma-Ray Astronomy VI*, SPIE, pp. 292–304.
- [22] Berry, B. S., and Pritchett, W. C., 1990, “Internal Stress and Internal Friction in Thin-layer Microelectronic Materials,” *Journal of Applied Physics*, **67**(8), pp. 3661–3668.
- [23] Acosta, R. E., Maldonado, J. R., Towart, L. K., and Warlaumont, J. M., 1984, “B-Si Masks for Storage Ring X-Ray Lithography,” *X-Ray Lithography and Applications of Soft X-Rays to Technology*, SPIE, pp. 114–118.
- [24] Karnezos, M., 1986, “Effects of Stress on the Stability of X-ray Masks,” *Journal of Vacuum Science & Technology B: Microelectronics Processing and Phenomena*, **4**(1), pp. 226–229.
- [25] Maden, M. A., Jagota, A., Mazur, S., and Farris, R. J., 1994, “Vibrational Technique for Stress Measurement in Films: I, Ideal Membrane Behavior,” *Journal of the American Ceramic Society*, **77**(3), pp. 625–635.
- [26] Su, C. M., and Wuttig, M., 1993, “In-Situ Mechanical Relaxation of Cu Films Growing on a Si Substrate,” *Applied Physics Letters*, **63**(25), pp. 3437–3439.
- [27] Berry, B. S., Pritchett, W. C., and Uzoh, C. E., 1989, “Dynamical Method for the Thermomechanical Study of Thin Membranes,” *Journal of Vacuum Science & Technology B: Microelectronics Processing and Phenomena*, **7**(6), pp. 1565–1569.
- [28] Su, C. M., Wen, Y., and Wuttig, M., 1996, “Internal Friction in Thin Films and Membrane,” *J. Phys. IV France*, **06**(C8), pp. C8-768.
- [29] Rayleigh, J. W. S., 1877, *The Theory of Sound*, London, Macmillan and co.
- [30] Ku, Y. C., Smith, H. I., and Plotnik, I., 1990, “Low Stress Tungsten Absorber for X-Ray Masks,” *Microelectronic Engineering*, **11**(1), pp. 303–308.
- [31] Whalen, M. M., 2023, “High-Precision Stress Measurement in Thin Films for X-Ray Mirrors,” Thesis, Massachusetts Institute of Technology.